NATIONAL ADVISORY COMMITTEE FOR AERONAUTICS

TECHNICAL NOTE 2021

BUCKLING OF THIN-WALLED CYLINDER UNDER AXIAL COMPRESSION AND INTERNAL PRESSURE

By Hsu Lo, Harold Crate, and Edward B. Schwartz

Langley Aeronautical Laboratory
Langley Air Force Base, Va.

Washington
January 1950

NATIONAL ADVISORY COMMITTEE FOR AERONAUTICS

TECHNICAL NOTE 2021

BUCKLING OF THIN-WALLED CYLINDER UNDER AXIAL COMPRESSION AND INTERNAL PRESSURE

By Hsu Lo, Harold Crate, and Edward B. Schwartz

SUMMARY

An investigation was made of a thin-walled cylinder under axial compression and various internal pressures to study the effect of the internal pressure on the compressive buckling stress of the cylinder. A theoretical analysis based on a large-deflection theory was also made. The theoretically predicted increase of compressive buckling stress due to internal pressure agrees fairly well with the experimental results.

INTRODUCTION

The buckling of thin-walled cylinders under axial compression and lateral pressure has been investigated by Flügge (reference 1) who found that the effect of the internal pressure on the buckling load is negligible. Flügge's conclusion is in contradiction to the results of a series of tests, made at the Langley Aeronautical Laboratory of the NACA, of two curved panels under axial compression and various lateral pressures. These test results, reported in reference 2, showed an appreciable strengthening effect of the lateral pressure on the buckling load of the curved panels. The apparent discrepancy between these experimental results and the prediction by Flügge's theory made it desirable to investigate this problem further. Consequently, additional tests were made of a cylinder under axial compression and various internal pressures for which results are presented herein. A theoretical analysis of this problem is also presented which differs from that of Flügge in that the present analysis is based on large, rather than small, deflection theory.

APPARATUS AND PROCEDURES

Test specimen.- The specimen used for the tests was a cylinder, 32 inches long with a 15-inch inside radius, made of 24S-T aluminum alloy sheet of 0.0249-inch average thickness. It was closely riveted around two heavy steel rings, one at each end. The butt-joint of the two longitudinal edges was covered both inside and outside by straps, 0.032 inch thick and $1\frac{1}{2}$ inch wide, along the total length of the cylinder. (See fig. 1.)

The two heavy steel rings were made of $\frac{1}{2}$- by 4-inch steel bar stock rolled to the diameter of the cylinder. Two $\frac{3}{8}$- by 2-inch spreader bars were used to reinforce the ring as shown in figure 1. A ring with a flange, machined flat, was fastened to the $\frac{1}{2}$- by 4-inch steel ring to provide an even bearing surface on which a steel cover plate was fitted. Three steel blocks were placed on top of the plate. The applied compressive load was transmitted from the machine head through the three steel blocks to the cover plate. The joint between the cylinder and the cover plates was sealed.

Equally spaced along the inside circumference of the cylinder at midlength were 16 strain gages, and directly opposite to them on the outside were 16 more gages. These gages were placed to measure strains in the longitudinal direction. Six more gages, three inside and three outside, were placed to measure the circumferential strains.

Test procedures.- The specimen was subjected to compressive load in the 1,200,000-pound universal testing machine of the Langley structures research laboratory. Compressed air was used to produce internal pressure, which could be maintained at any desired constant value. The pressure was measured by a manometer. The strains were recorded by standard electric strain-gage equipment and the end-shortening was measured by dial gages.

The cylinder was preloaded and the strain-gage readings were taken. The three steel blocks were so adjusted that all longitudinal strain-gage readings around the circumference of the cylinder were equal.

The compressed air was then let into the cylinder until the desired internal pressure was reached. The axial compressive load was increased in increments until buckling was observed. At each load increment, all gage readings were recorded. The load was then decreased

until the buckles disappeared and increased a second time to check the reading obtained the first time. During all these steps the internal pressure was maintained constant.

The axial load was then reduced and the internal pressure was changed to another value. For each value of internal pressure the same procedure was repeated.

EXPERIMENTAL RESULTS

A typical experimental result is shown in figures 2(a) and 2(b) for the case in which the internal pressure was $1\frac{1}{2}$ psi. In figure 2(a) the compressive load is plotted against the strain-gage readings for four different pairs of gages, within the range where the load-strain relation is linear. In figure 2(b) the strain-gage reading is plotted for all strain gages at three compressive loadings close to the buckling load. Figure 2(b) indicates that buckling occurs at a compressive load of 12,700 pounds between strain gages 22 and 23. (Note the intersection of the curves at two consecutive loadings.) A buckle at this location was observed during the test. The compressive load at which this phenomenon occurs is considered the buckling load.

Since the buckling occurs locally and not simultaneously at all the gages, the local buckling strain is obtained by dividing the buckling load by the slope of the linear portion of the load-strain curve corresponding to the gage at which the buckling occurs. The corresponding stress is the buckling stress. The buckling stresses for various internal pressures were determined in this same way.

The results are tabulated in table 1 and plotted in figure 3 in terms of the two nondimensional parameters

$$\bar{\sigma}_{cr} = \frac{\sigma_{u_{cr}}}{E}\frac{R}{t}$$

$$\bar{p} = \frac{p}{E}\left(\frac{R}{t}\right)^2$$

where $\sigma_{u_{cr}}$ is the buckling stress, p is the internal pressure, R is the radius of the cylinder, t is the wall thickness, and E is Young's modulus. Except for the first test corresponding to $\bar{p} = 0.1028$ in which the cylinder had undergone no previous buckling, all the tests were carried out on the cylinder with possible permanent set.

THEORETICAL RESULTS

A theoretical analysis for calculating the buckling stress of a cylindrical shell under axial compression and internal pressure was obtained by a "large-deflection" theory for which details are given in the appendix. The large-deflection theory was first advanced by Von Kármán and Tsien (reference 3) in the study of buckling stress of cylindrical shells under axial compression (but without internal pressure). This theory was subsequently improved by Leggett and Jones (reference 4). In reference 3 the buckling stress was shown to depend on whether the load was applied by a rigid loading machine or by a dead-weight machine. In the present analysis, the loading machine is assumed to be rigid.

The existing procedures for computation of the buckling stress by large-deflection theory involve the solution of four simultaneous nonlinear equations for each pressure loading. The numerical work is quite lengthy. The method used in the present study introduces a fifth equation which governs the conditions at which the buckling occurs. The fifth equation is based on consideration of conservation of energy, which is an extension of Tsien's buckling criterion given in reference 5. Although a solution of five simultaneous equations is now necessary, the numerical work is actually reduced to a small fraction of that required if the existing procedures were used. This reduction in labor is made possible through a proper choice of the parameters in the equations and the process of the computations. The results calculated by the present method are presented in table 1 and are represented by the solid-line curve in figure 3. The curve is cut off at a value of $\bar{\sigma}_{cr} = 0.605$, corresponding to $\bar{p} \approx 0.169$. This constant value of $\bar{\sigma}_{cr} = 0.605$ for $\bar{p} > 0.169$ is the same that is obtained by the classical theory.

DISCUSSION AND CONCLUSIONS

From the theoretical and experimental results shown in figure 3, the internal pressure is seen to have an appreciable strengthening effect on the cylinder. Although the two curves obtained from theoretical and experimental results do not coincide, both show the same trends as regards the effect of internal pressure on the buckling stresses. If the increment of the buckling stress $\Delta\bar{\sigma}_{cr}$ due to the presence of internal pressure (that is, the difference between the buckling stress with the pressure $\bar{\sigma}_{cr}$ and that without the pressure $(\bar{\sigma}_{cr})_{\bar{p}=0}$) is plotted against the internal pressure, as shown in figure 4, a good agreement is obtained between the theoretical and experimental results. These data indicate that, although further improvement of the theory

is necessary for the determination of the magnitude of the compressive buckling stress, the theory gives a fairly good prediction of the increase of compressive buckling stress that may be expected as a result of internal pressure. The discrepancy between the theoretical curve and the experimental curve of figure 3 is believed to be caused by such factors as manufacturing imperfections in the specimens, material irregularities, and energy absorbed by the loading machine, which have not been included in the theory.

Langley Aeronautical Laboratory
National Advisory Committee for Aeronautics
Langley Air Force Base, Va.

APPENDIX

THEORETICAL ANALYSIS OF BUCKLING LOAD OF CYLINDRICAL SHELLS UNDER AXIAL COMPRESSION AND INTERNAL PRESSURE BY LARGE-DEFLECTION THEORY

Background of Theory

The use of large-deflection theory for shells under axial compression was first advanced by Von Kármán and Tsien (reference 3) in an attempt to explain the discrepancies between the buckling loads predicted by classical theory and those obtained from experimental results. (See for instance, reference 6.) The results of reference 3 indicated that cylindrical shells can be maintained in equilibrium in the buckled state by a compressive load considerably lower than that predicted by classical theory. A plausible explanation of this result is that, before the classical buckling load is reached during a test, the cylindrical shell "jumps" from an equilibrium unbuckled state to an equilibrium buckled state. The physical phenomena of the jump were further examined in reference 5 by Tsien.

The treatment of Von Kármán and Tsien in reference 3 was left incomplete, however, in that the equilibrium positions at the buckled state were determined by differentiating the total potential energy with respect to some but not all of the physical parameters involved. The resulting equations gave a relation between the average compressive stress σ and the end-shortening ϵ in terms of the remaining parameters. A set of curves of σ against ϵ were thus obtained for various combinations of the remaining parameters.

Improvement of Von Kármán and Tsien's theory was made by Leggett and Jones (reference 4), who took the derivatives of the energy with respect to all the parameters and thus obtained a single curve between σ and ϵ, representing all equilibrium positions of the cylindrical shell in the buckled state. The same result was obtained by Michielsen (reference 7) in a similar process. Such a curve is shown by BC of figure 5.

Theoretically, when the cylinder is compressed, the relation between σ and ϵ follows the straight line ODA which represents the unbuckled state and will reach the point A if everything is perfect; the cylinder then buckles and the relationship follows the curve ABC which represents the buckled state. Before point A is reached, however, some external disturbance may possibly cause the cylinder to jump from

the unbuckled state represented by the point D to the buckled state represented by the point E. The positions of D and E on the respective curves depend on the actual physical conditions of the jump.

If the physical condition which governs the jump is known or defined, the buckling stress corresponding to the point D can be obtained directly without going through the labor of finding the curve ABC. This procedure can greatly reduce the amount of numerical work.

In reference 5, Tsien introduced a criterion which governs the jump DE for the condition of loading obtained in a rigid testing machine, namely, that the strain energy remains the same before and after the jump and that the jump occurs at constant end-shortening. According to this criterion the line DE must be vertical and must cut the curve AB in such a way that the two shaded areas ADG and GBE are equal. In fact, the area ADG represents the additional energy that is needed to assist the cylinder in jumping from a condition represented by D to that represented by G and the area GBE represents the energy that is given up by the cylinder when it arrives at the lower energy level, point E. The energy represented by the area ADG is very small, and therefore a slight disturbance from the surrounding air might assist the cylinder to jump from the unbuckled state to the buckled state at a compressive stress well below the classical buckling stress corresponding to point A.

Since the external disturbance is required to assist the cylinder to jump from the state corresponding to D to that corresponding to G, a slightly larger external disturbance can well cause the cylinder to make the transition from the state represented by D' to that represented by B, except that in the case in which the cylinder jumps from D' to B the cylinder absorbs the energy of the external disturbance and does not reemit it. The buckling stress can be then as low as point D'. This fact was pointed out by Tsien in reference 8.

In addition to the two criterions just mentioned, there are still others that might be used. In view of the fact that the choice of the buckling criterion is a much less important factor in the determination of buckling stress than are such other factors as, for example, the initial imperfections, Tsien's criterion of reference 5, as represented by the line DE, is as reasonable as any other, and the choice of this criterion greatly simplifies the numerical work.

Tsien's criterion of reference 5 cannot be applied directly to the present analysis, however, because with the presence of the internal pressure the strain energy is no longer the same before and after the jump. In addition, the criterion is applied herein in quite a different manner from that of reference 5. In reference 5, a series of values of wave number n and aspect ratio β were chosen and the criterion was applied to each pair of values of n and β; the pair of values of n

and β which gave the minimum value of buckling load was considered to correspond to the buckling condition. In the present analysis, since the variation of σ with ϵ can be plotted only as a single curve, this criterion need be applied only once for each internal pressure. The results correspond to the minimum-potential-energy condition.

In the derivation of the present analysis, the basic equations in reference 3 are first extended to include the effect of internal pressure, Tsien's criterion governing the jump for rigid machine loading (reference 5) is modified, and the buckling stress is finally obtained.

Symbols

A list of symbols follows. Most of the symbols used in the present paper are the same as those in reference 3; exceptions are the use of μ for Poisson's ratio, λ for wave length, and β for aspect ratio of the buckled waves.

λ_a	half wave length in longitudinal direction
λ_b	half wave length in circumferential direction
f_0, f_1, f_2	parameters used in deflection function
m	number of waves in longitudinal direction within length equal to circumference of cylinder
n	number of waves in circumference
p	internal pressure
t	thickness of cylinder wall
x,y	coordinates measured in longitudinal and circumferential directions, respectively
u	component of displacement of a point on median surface of shell in x-direction
w	component of displacement of a point on median surface of shell in radial direction
α	measure of average circumferential stress per wave length in longitudinal direction
ϵ	end-shortening of cylinder

σ	average compressive stress
$\beta = \frac{m}{n}$	aspect ratio of buckled waves
μ	Poisson's ratio
ϕ	total potential energy
E	Young's modulus
ψ	strain energy
$B_1, B_2, \ldots B_6$ $B_1', B_2', \ldots B_6'$	certain functions of β
$D_1, D_2, \ldots D_5$	certain functions of ρ and β
$(D)_\rho = \frac{\partial D}{\partial \rho}$	(D represents the functions $D_1, D_2, \ldots D_5$)
$(D)_\beta = \beta \frac{\partial D}{\partial \beta}$	(D represents the functions $D_1, D_2, \ldots D_5$)
R	radius of cylinder
W_1	elastic extensional energy
W_2	bending energy
W_3	work done by applied compressive load
W_p	work done by internal pressure

Nondimensional parameters:

$$\rho = \frac{f_2}{f_1}$$

$$\zeta = f_1 \frac{R}{t}$$

$$\eta = n^2 \frac{t}{R}$$

$$\bar{\sigma} = \frac{\sigma}{E} \frac{R}{t}$$

$$\bar{p} = \frac{p}{t}\left(\frac{R}{t}\right)^2$$

$$\bar{W} = \frac{W}{\frac{1}{2}Et\lambda_a\lambda_b}$$ ($\bar{W}_1$, $\bar{W}_2$, $\bar{W}_3$, and $\bar{W}_p$ are defined in the same manner.)

$$\bar{\phi} = \frac{\phi}{\frac{1}{2}Et\lambda_a\lambda_b}$$

$$\bar{\psi} = \frac{\psi}{\frac{1}{2}Et\lambda_a\lambda_b}$$

$$\bar{\epsilon} = \epsilon\frac{R}{t}$$

$$\bar{\sigma}' = \left(\bar{\sigma} - \frac{1}{\beta^2}\bar{p}\right)\eta D_1$$

Subscripts:

o	pertaining to buckling condition
u	unbuckled state just prior to buckling
cr	buckling condition

Derivation of Basic Equations

Three basic equations are derived in the following analysis to include the effect of internal pressure. They are the expression for the total potential energy, the expression for the strain energy, and the relation between the end-shortening and the average compressive stress.

In order to calculate the total potential energy, the work done by the internal pressure should be included in addition to the energies W_1, W_2, and W_3, which are given by equations (25), (26), and (27) of reference 3 as:

$$\frac{W_1}{\frac{1}{2}Et\lambda_a\lambda_b} = 4\left[\left(1 - \mu^2\right)\left(\frac{\sigma}{E}\right)^2 + n^4\left(\frac{3}{64}f_1^2 + \frac{1}{16}f_1f_2 + \frac{1}{16}f_2^2\right)^2 + \left(f_0 + \frac{1}{4}f_1\right)^2 - 2n^2\left(\frac{3}{64}f_1^2 + \frac{1}{16}f_1f_2 + \frac{1}{16}f_2^2\right)\left(f_0 + \frac{1}{4}f_1\right)\right] + \left[\frac{A^2}{8} + \frac{B^2\beta^4}{8} + \frac{\beta^4C^2}{(1 + \beta^2)^2} + \frac{\beta^4D^2}{(1 + 9\beta^2)^2} + \frac{\beta^4G^2}{(9 + \beta^2)^2} + \frac{\beta^4H^2}{16(1 + \beta^2)^2}\right] \quad (1)$$

$$\frac{W_2}{\frac{1}{2}Et\lambda_a\lambda_b} = \frac{1}{6(1-\mu^2)}\left(\frac{t}{R}\right)^2 n^4 \left\{ f_1^2 \left[\frac{1}{8}(1+\beta^2)^2 + \frac{1}{4}(1+\beta^4) \right] + (1+\beta^4) f_1 f_2 + (1+\beta^4) f_2^2 \right\} \tag{2}$$

$$\frac{W_3}{\frac{1}{2}Et\lambda_a\lambda_b} = \left[2(1-\mu^2)\left(\frac{g}{E}\right)^2 + n^2 \frac{g}{E}(\mu+\beta^2)\left(\frac{3}{32}f_1^2 + \frac{1}{8}f_1 f_2 + \frac{1}{8}f_2^2\right) - 2\mu\frac{g}{E}\left(f_0 + \frac{1}{4}f_1\right) \right] \tag{3}$$

where a, b, μ, and ν have been changed to λ_a, λ_b, β, and μ, respectively, to agree with the notation of the present paper and where

$$A = \frac{1}{8}f_1^2 n^2 - \left(\frac{1}{2}f_1 + f_2\right)$$

$$B = \frac{1}{8}f_1^2 n^2$$

$$C = \frac{1}{2}f_1 n^2\left(\frac{1}{2}f_1 + f_2\right) - \frac{1}{2}f_1$$

$$D = \frac{1}{4}f_1 n^2\left(\frac{1}{2}f_1 + f_2\right)$$

$$G = \frac{1}{4}f_1 n^2\left(\frac{1}{2}f_1 + f_2\right)$$

and

$$H = n^2\left(\frac{1}{2}f_1 + f_2\right)^2$$

The work done by the internal pressure is, for a complete wave panel,

$$W_p = -4\int_0^{\lambda_a}\int_0^{\lambda_b} wp\, dx\, dy$$

The negative sign is introduced because the radial deflection w is considered positive inward.

If the same deflection function given in equation (16) of reference 3 is used, that is,

$$\frac{w}{R} = \left(f_0 + \frac{f_1}{4}\right) + \frac{f_1}{2}\left(\cos\frac{mx}{R}\cos\frac{ny}{R} + \frac{1}{4}\cos\frac{2mx}{R} + \frac{1}{4}\cos\frac{2ny}{R}\right) + \frac{f_2}{4}\left(\cos\frac{2mx}{R} + \cos\frac{2ny}{R}\right) \tag{4}$$

the work done by the internal pressure becomes

$$W_p = -4pR\lambda_a\lambda_b\left(f_0 + \frac{f_1}{4}\right) \tag{5}$$

If the total potential energy

$$\phi = W_1 + W_2 - W_3 - W_p$$

is differentiated with respect to f_0 and the derivative is set equal to zero, the following expression is obtained

$$f_0 + \frac{f_1}{4} = \frac{1}{16}n^2\left(\frac{3}{4}f_1^2 + f_1f_2 + f_2^2\right) - \mu\frac{\sigma}{E} - \frac{pR}{Et} \tag{6}$$

Substitute this expression into equations (1), (2), (3), and (5) for W_1, W_2, W_3, and W_p, respectively, and the following equations are obtained:

$$\frac{W_1}{\frac{1}{2}Et\lambda_a\lambda_b} = 4\left[\left(\frac{\sigma}{E}\right)^2 + 2\mu\left(\frac{\sigma}{E}\right)\left(\frac{pR}{Et}\right) + \left(\frac{pR}{Et}\right)^2\right] + n^4\left(B_1f_1^4 + B_2f_1^3f_2 + B_3f_1^2f_2^2 + B_4f_1f_2^3 + \frac{B_4}{2}f_2^4\right) - n^2\left[\left(2B_4 + \frac{1}{64}\right)f_1^3 + \left(4B_4 + \frac{1}{32}\right)f_1^2f_2\right] + \left[\left(2B_4 + \frac{1}{32}\right)f_1^2 + \frac{1}{8}f_1f_2 + \frac{1}{8}f_2^2\right] \tag{7}$$

$$\frac{W_2}{\frac{1}{2}Et\lambda_a\lambda_b} = \left(\frac{t}{R}\right)^2\left(B_5f_1^2 + B_6f_1f_2 + B_6f_2^2\right)n^4 \tag{8}$$

$$\frac{W_3}{\frac{1}{2}Et\lambda_a\lambda_b} = 4\left[2\left(\frac{\sigma}{E}\right)^2 + 2\mu\left(\frac{\sigma}{E}\right)\left(\frac{pR}{Et}\right) + \frac{1}{8}\left(\frac{\sigma}{E}\right)n^2\beta^2\left(\frac{3}{4}f_1^2 + f_1f_2 + f_2^2\right)\right] \tag{9}$$

$$\frac{W_p}{\frac{1}{2}Et\lambda_a\lambda_b} = 8\left[\left(\frac{pR}{Et}\right)^2 + 8\mu\left(\frac{\sigma}{E}\right)\left(\frac{pR}{Et}\right) - n^2\left(\frac{pR}{Et}\right)\frac{1}{16}\left(\frac{3}{4}f_1^2 + f_1f_2 + f_2^2\right)\right] \tag{10}$$

where

$$B_1 = \frac{1}{64}\left[\frac{1+\beta^4}{8} + \frac{17}{4}\frac{\beta^4}{(1+\beta^2)^2} + \frac{\beta^4}{(1+9\beta^2)^2} + \frac{\beta^4}{(9+\beta^2)^2}\right]$$

$$B_2 = \frac{1}{16}\left[\frac{9}{2}\frac{\beta^4}{(1+\beta^2)^2} + \frac{\beta^4}{(1+9\beta^2)^2} + \frac{\beta^4}{(9+\beta^2)^2}\right]$$

$$B_3 = \frac{1}{16}\left[\frac{11}{2}\frac{\beta^4}{(1+\beta^2)^2} + \frac{\beta^4}{(1+9\beta^2)^2} + \frac{\beta^4}{(9+\beta^2)^2}\right]$$

$$B_4 = \frac{1}{8}\frac{\beta^4}{(1+\beta^2)^2}$$

$$B_5 = \frac{1}{6(1-\mu^2)}\left[\frac{1}{8}(1+\beta^2)^2 + \frac{1}{4}(1+\beta^4)\right]$$

$$B_6 = \frac{1}{6(1-\mu^2)}(1+\beta^4)$$

Equations (7) to (10) may be expressed in terms of the nondimensional parameters $\bar{\sigma}$, $\bar{p}$, ρ, η, ζ, and $\bar{W}$ as

$$\bar{W}_1 = 4\left(\bar{\sigma}^2 + 2\mu\bar{\sigma}\bar{p} + \bar{p}^2\right) + \eta^2\zeta^4 D_2 + \eta\zeta^3(-D_3) + \zeta^2 D_4 \tag{11}$$

$$\bar{W}_2 = \eta^2\zeta^2 D_5 \tag{12}$$

$$\bar{W}_3 = 8\bar{\sigma}^2 + 8\mu\bar{\sigma}\bar{p} + \bar{\sigma}\eta\zeta^2 D_1 \tag{13}$$

$$\bar{W}_p = 8\mu\bar{\sigma}\bar{p} + 8\bar{p}^2 - \frac{1}{\beta^2}\bar{p}\eta\zeta^2 D_1 \tag{14}$$

where

$$D_1 = \frac{1}{2}\beta^2\left(\frac{3}{4} + \rho + \rho^2\right)$$

$$D_2 = B_1 + B_2\rho + B_3\rho^2 + B_4\rho^3 + \frac{1}{2}B_4\rho^4$$

$$D_3 = \left(2B_4 + \frac{1}{64}\right)(1 + 2\rho)$$

$$D_4 = \left(2B_4 + \frac{1}{32}\right) + \frac{1}{8}(\rho + \rho^2)$$

$$D_5 = B_5 + B_6(\rho + \rho^2)$$

The nondimensional total-potential-energy parameter $\bar{\phi}$ is

$$\begin{aligned}\bar{\phi} &= \bar{W}_1 + \bar{W}_2 - \bar{W}_3 - \bar{W}_p \\ &= -4(\bar{\sigma}^2 + 2\mu\bar{\sigma}\bar{p} + \bar{p}^2) - \left(\bar{\sigma} - \frac{1}{\beta^2}\bar{p}\right)\eta\zeta^2 D_1 + \\ &\quad \eta^2\zeta^4 D_2 - \eta\zeta^3 D_3 + \zeta^2 D_4 + \eta^2\zeta^2 D_5\end{aligned} \tag{15}$$

The nondimensional strain-energy parameter $\bar{\Psi}$ is

$$\bar{\Psi} = \bar{W}_1 + \bar{W}_2$$

$$= 4(\bar{\sigma}^2 + 2\mu\bar{\sigma}\bar{p} + \bar{p}^2) + \eta^2\zeta^4 D_2 -$$

$$\eta\zeta^3 D_3 + \zeta^2 D_4 + \eta^2\zeta^2 D_5$$

The relation between the end-shortening ϵ and the average compressive stress can be determined from equation (23) of reference 3 by integrating; thus,

$$\epsilon = -\frac{1}{\lambda_a}\int_0^{\lambda_a} \frac{\partial u}{\partial x}\, dx$$

$$= \left(\frac{\sigma}{E} + \mu\frac{\alpha}{E}\right) + \frac{1}{16}\eta^2\beta^2\left(\frac{3}{4}f_1^2 + f_2^2 + f_1 f_2\right)$$

where α/E, as determined from equation (24) of reference 3, together with equation (6) herein is

$$\frac{\alpha}{E} = \frac{pR}{Et}$$

Therefore, the relation between $\bar{\epsilon}$ and $\bar{\sigma}$ in nondimensional form becomes

$$\bar{\epsilon} = \epsilon\frac{R}{t}$$

$$= \bar{\sigma} + \mu\bar{p} + \frac{1}{8}\eta\zeta^2 D_1 \qquad (17)$$

Equations (15), (16), and (17) are for cylinders in the buckled state. For cylinders in the unbuckled state, the corresponding equations are

$$\bar{\phi}_u = -4(\bar{\sigma}_u^2 + 2\mu\bar{\sigma}_u\bar{p} + \bar{p}^2) \tag{18}$$

$$\bar{\psi}_u = 4(\bar{\sigma}_u^2 + 2\mu\bar{\sigma}_u\bar{p} + \bar{p}^2) \tag{19}$$

$$\bar{\epsilon}_u = \bar{\sigma}_u + \mu\bar{p} \tag{20}$$

Equilibrium Positions of Cylinders in Buckled State

The equilibrium positions of cylinders in the buckled state can be obtained by differentiating the total potential energy of equation (15) with respect to each of the parameters η, ζ, ρ, and β and by setting the derivatives equal to zero. Four simultaneous, nonlinear equations are thus obtained:

$$\left.\begin{aligned}
\frac{\partial\bar{\phi}}{\partial\eta} = 0 &= -\left[\left(\bar{\sigma} - \frac{1}{\beta^2}\bar{p}\right)\eta D_1 - 2(\eta\zeta)^2 D_2 + (\eta\zeta)D_3 - 2\eta^2 D_5\right]\left(\frac{\zeta^2}{\eta}\right) \\
\frac{\partial\bar{\phi}}{\partial\zeta} = 0 &= -\left[\left(\bar{\sigma} - \frac{1}{\beta^2}\bar{p}\right)\eta D_1 - 2(\eta\zeta)^2 D_2 + 1.5(\eta\zeta)D_3 - D_4 - \eta^2 D_5\right](2\zeta) \\
\frac{\partial\bar{\phi}}{\partial\rho} = 0 &= -\left[\left(\bar{\sigma} - \frac{1}{\beta^2}\bar{p}\right)\eta(D_1)_\rho - (\eta\zeta)^2(D_2)_\rho + (\eta\zeta)(D_3)_\rho - (D_4)_\rho - \eta^2(D_5)_\rho\right]\zeta^2 \\
\frac{\partial\bar{\phi}}{\partial\beta} = 0 &= -\left[\left(\bar{\sigma} - \frac{1}{\beta^2}\bar{p}\right)\eta(D_1)_\beta - (\eta\zeta)^2(D_2)_\beta + (\eta\zeta)(D_3)_\beta - (D_4)_\beta - \eta^2(D_5)_\beta + \frac{2}{\beta^2}\bar{p}\eta D_1\right]\frac{\zeta^2}{\beta}
\end{aligned}\right\} \tag{21}$$

where

$$(D_1)_\rho = \frac{1}{2}\beta^2(1 + 2\rho)$$

$$(D_2)_\rho = B_2 + 2B_3\rho + 3B_4\rho^2 + 2B_4\rho^3$$

$$(D_3)_\rho = 2\left(B_4 + \frac{1}{64}\right)$$

$$(D_4)_\rho = \frac{1}{8}(1 + 2\rho)$$

$$(D_5)_\rho = B_6(1 + 2\rho)$$

$$(D_1)_\beta = \beta^2\left(\frac{3}{4} + \rho + \rho^2\right) = 2D_1$$

$$(D_2)_\beta = B_1' + B_2'\rho + B_3'\rho^2 + B_4'\rho^3 + \frac{1}{2}B_4'\rho^4$$

$$(D_3)_\beta = 2B_4'(1 + 2\rho)$$

$$(D_4)_\beta = 2B_4'$$

$$(D_5)_\beta = B_5' + B_6'(\rho + \rho^2)$$

and

$$B_1' = \frac{1}{16}\left[\frac{\beta^4}{8} + \frac{17}{4}\frac{\beta^4}{(1 + \beta^2)^3} + \frac{\beta^4}{(1 + 9\beta^2)^3} + 9\frac{\beta^4}{(9 + \beta^2)^3}\right]$$

$$B_2' = \frac{1}{4}\left[\frac{9}{2}\frac{\beta^4}{(1 + \beta^2)^3} + \frac{\beta^4}{(1 + 9\beta^2)^3} + 9\frac{\beta^4}{(9 + \beta^2)^3}\right]$$

$$B_3' = \frac{1}{4}\left[\frac{11}{2}\frac{\beta^4}{(1 + \beta^2)^3} + \frac{\beta^4}{(1 + 9\beta^2)^3} + 9\frac{\beta^4}{(9 + \beta^2)^3}\right]$$

$$B_4' = \frac{1}{2}\frac{\beta^4}{(1 + \beta^2)^3}$$

$$B_5' = \frac{1}{6(1 - \mu^2)} \frac{1}{2}\beta^2(1 + 3\beta^2)$$

$$B_6' = \frac{4}{6(1 - \mu^2)}\beta^4$$

Let

$$\bar{\sigma}' = \left(\bar{\sigma} - \frac{1}{2}\bar{p}\right)\eta D_1$$

The four simultaneous equations (21) become

$$\bar{\sigma}' = (\eta\zeta)^2(2D_2) - (\eta\zeta)D_3 + 2\eta^2 D_5 \tag{22a}$$

$$\bar{\sigma}' = (\eta\zeta)^2(2D_2) - (\eta\zeta)(1.5D_3) + D_4 + \eta^2 D_5 \tag{22b}$$

$$\bar{\sigma}' = \left[(\eta\zeta)^2(D_2)_\rho - (\eta\zeta)(D_3)_\rho + (D_4)_\rho + \eta^2(D_5)_\rho\right]\frac{D_1}{(D_1)_\rho} \tag{22c}$$

$$\bar{\sigma}' = \left[(\eta\zeta)^2(D_2)_\beta - (\eta\zeta)(D_3)_\beta + (D_4)_\beta + \eta^2(D_5)_\beta\right]\frac{1}{2} - \frac{\bar{p}}{\beta^2}\eta D_1 \tag{22d}$$

Theoretically these four simultaneous equations can be solved for η, ζ, ρ, and β in terms of $\bar{\sigma}$ for a given pressure. If they are substituted into equation (17), a relation between end-shortening $\bar{\epsilon}$ and the compressive stress $\bar{\sigma}$ is obtained which represents all equilibrium positions at the buckled state. In fact, this solution is essentially that obtained by Leggett and Jones (reference 4) and Michielsen (reference 7) for cylinders with axial compression but no internal pressure.

Practically, however, the solution of the four simultaneous equations (22) requires a long and tedious numerical process. If only the buckling stress is required, calculation of only one point on the curve of $\bar{\sigma}$ against $\bar{\epsilon}$ rather than the whole curve is necessary. This solution can be obtained by the introduction of one more equation which governs the condition at buckling.

Buckling Criterion

In reference 5, Tsien gave the following criterion which governs the condition at buckling: That the strain-energy of the buckled cylinder is the same as the strain energy of the unbuckled cylinder when the cylinder is tested in the rigid testing machine so that the end-shortening does not change during buckling. This criterion is apparently established from considerations of conservation of energy. Although other physical criterions can be used (for instance, see reference 8), the criterion of reference 5 was chosen and extended to include the case for which the internal pressure is present. The choice of this criterion simplifies the numerical work.

When internal pressure is present in the cylinder, work is done by the pressure during buckling. The strain energy in the buckled state is no longer equal to that in the unbuckled state, but

$$\bar{\Psi} = \bar{\Psi}_u + \Delta\bar{W}_p \tag{23}$$

where $\Delta\bar{W}_p$ is the work done by the pressure during buckling, or

$$\Delta\bar{W}_p = \frac{1}{\frac{1}{2}Et\lambda_a\lambda_b}\left(\frac{R}{t}\right)^2\left[-\int_0^{\lambda_a}\int_0^{\lambda_b} p(w - w_u)\,dx\,dy\right]$$

$$= \bar{W}_p - (\bar{W}_p)_u \tag{24}$$

Equation (14) can be rearranged as follows:

$$\bar{W}_p = 8(\bar{p}^2 + \mu\bar{\sigma}\bar{p}) - \frac{1}{\beta^2}\bar{p}\eta\zeta^2 D_1 \tag{25}$$

Therefore, for the unbuckled state, the last term is eliminated and

$$(\bar{W}_p)_u = 8(\bar{p}^2 + \mu\bar{\sigma}_u\bar{p}) \tag{26}$$

Then, from equations (24), (25), and (26)

$$\Delta\bar{W}_p = 8\mu\bar{p}(\bar{\sigma} - \bar{\sigma}_u) - \frac{1}{\beta^2}\bar{p}\eta\zeta^2 D_1 \tag{27}$$

The buckling criterion becomes (equations (23) and (27))

$$\bar{\psi} = \bar{\psi}_u + 8\mu\bar{p}(\bar{\sigma} - \bar{\sigma}_u) - \frac{1}{\beta^2}\bar{p}\eta\zeta^2 D_1$$

or, from equations (16) and (19),

$$4(\bar{\sigma}^2 + 2\mu\bar{\sigma}\bar{p} + \bar{p}^2) + \eta^2\zeta^4 D_2 - \eta\zeta^3 D_3 + \zeta^2 D_4 + \eta^2\zeta^2 D_5$$

$$= 4(\bar{\sigma}_u^2 + 2\mu\bar{\sigma}_u\bar{p} + \bar{p}^2) + 8(\bar{\sigma} - \bar{\sigma}_u)\mu\bar{p} - \frac{1}{\beta^2}\bar{p}\eta\zeta^2 D_1 \qquad (28)$$

Since the end-shortening remains unchanged during buckling, that is, $\bar{\epsilon} = \bar{\epsilon}_u$, the following relation is obtained from equations (17) and (20).

$$\bar{\sigma}_u = \bar{\sigma} + \frac{1}{8}\eta\zeta^2 D_1 \qquad (29)$$

If this relation is substituted in equation (28) and if the relation $\bar{\sigma}' = \left(\bar{\sigma} - \frac{1}{\beta^2}\bar{p}\right)\eta D_1$ is used, the buckling criterion becomes

$$\bar{\sigma}' = (\eta\zeta)^2\left(D_2 - \frac{1}{16}D_1^2\right) - (\eta\zeta)D_3 + D_4 + \eta^2 D_5 \qquad (30)$$

The solution of the five equations (22a), (22b), (22c), (22d), and (30) gives the buckling stress for a given internal pressure. The following section presents a very simple method for the solution of these five simultaneous equations.

Method of Solution

From equations (22b) and (30) and equations (22a) and (22b), the following equations are obtained:

$$\eta\zeta = \frac{D_3}{2\left(D_2 + \frac{1}{16}D_1^2\right)} \qquad (31)$$

$$\eta^2 = \frac{D_4 - \frac{1}{2}D_3(\eta\zeta)}{D_5} \qquad (32)$$

For a preassigned value of β, assume various values of ρ and compute $\eta\zeta$ and η^2 from equations (31) and (32). Substitute these values in equations (22a) and (22c) to obtain $(\bar{\sigma}')_a$ and $(\bar{\sigma}')_c$, respectively. Plot both $(\bar{\sigma}')_a$ and $(\bar{\sigma}')_c$ against ρ. The intersection of these two curves determines a pair of values $\bar{\sigma}'$ and ρ which are called $\bar{\sigma}'_o$ and ρ_o. The corresponding $(\eta\zeta)_o$ and $(\eta^2)_o$ are computed and substituted in equation (22d) from which the pressure $\bar{p}$ can be calculated. For each assigned value of β, there are obtained corresponding values of $\bar{\sigma}'_o$ and $\bar{p}$. A curve of $\bar{\sigma}'_o$ against $\bar{p}$ can thus be determined. If the following relations are used,

$$\bar{\sigma}'_o = (\eta D_1)_o\left(\bar{\sigma}_o - \frac{1}{\beta^2}\bar{p}\right)$$

$$\bar{\sigma}_{cr} = (\bar{\sigma}_u)_o = \bar{\sigma}_o + \frac{1}{8}(\eta\zeta^2 D_1)_o$$

the relation between $\bar{\sigma}_{cr}$ and $\bar{p}$ is obtained as shown in figure 3.

Cut-Off Buckling Stress

When equation (31) is derived from equations (22b) and (30), a factor $(\eta\zeta) = 0$ is also obtained. If this relation is used instead of equation (31), it can be shown that the buckling stress $\bar{\sigma}_{cr}$ can never exceed the classical buckling stress 0.605 which is independent of pressure.

REFERENCES

1. Flügge, W.: Die Stabilität der Krieszylinderschale. Ing.-Archiv, Bd. III, Heft 5, Dec. 1932, pp. 463-506.

2. Rafel, Norman: Effect of Normal Pressure on the Critical Compressive Stress of Curved Sheet. NACA RB, Nov. 1942.

3. Von Kármán, Theodore, and Tsien, Hsue-Shen: The Buckling of Thin Cylindrical Shells under Axial Compression. Jour. Aero. Sci., vol. 8, no. 8, June 1941, pp. 303-312.

4. Leggett, D. M. A., and Jones, R. P. N.: The Behavior of a Cylindrical Shell under Axial Compression When the Buckling Load Has Been Exceeded. R. & M. No. 2190, British A.R.C., 1942.

5. Tsien, Hsue-Shen: A Theory for the Buckling of Thin Shells. Jour. Aero. Sci., vol. 9, no. 10, Aug. 1942, pp. 373-384.

6. Lundquist, Eugene E.: Strength Tests of Thin-Walled Duralumin Cylinders in Compression. NACA Rep. 473, 1933.

7. Michielsen, Herman F.: The Behavior of Thin Cylindrical Shells after Buckling under Axial Compression. Jour. Aero. Sci., vol. 15, no. 12, Dec. 1948, pp. 738-744.

8. Tsien, Hsue-Shen: Lower Buckling Load in the Non-Linear Buckling Theory for Thin Shells. Quarterly Appl. Math., vol. V, no. 2, July 1947, pp. 236-237.

TABLE 1

BUCKLING STRESSES FOR VARIOUS INTERNAL PRESSURES

Experimental			Theoretical		
$\bar{p}$	$\bar{\sigma}$	$\Delta\bar{\sigma}_{cr}$	$\bar{p}$	$\bar{\sigma}$	$\Delta\bar{\sigma}_{cr}$
0	0.1936	0	0	0.376	0
.01715	.252	.058	.02	.444	.068
.03425	.277	.083	.04	.480	.104
.0514	.309	.116	.06	.506	.130
.0685	.350	.156	.08	.528	.152
.0856	.363	.170	.10	.547	.171
.1028	.407	.213	.12	.565	.189
			.14	.581	.205

NACA

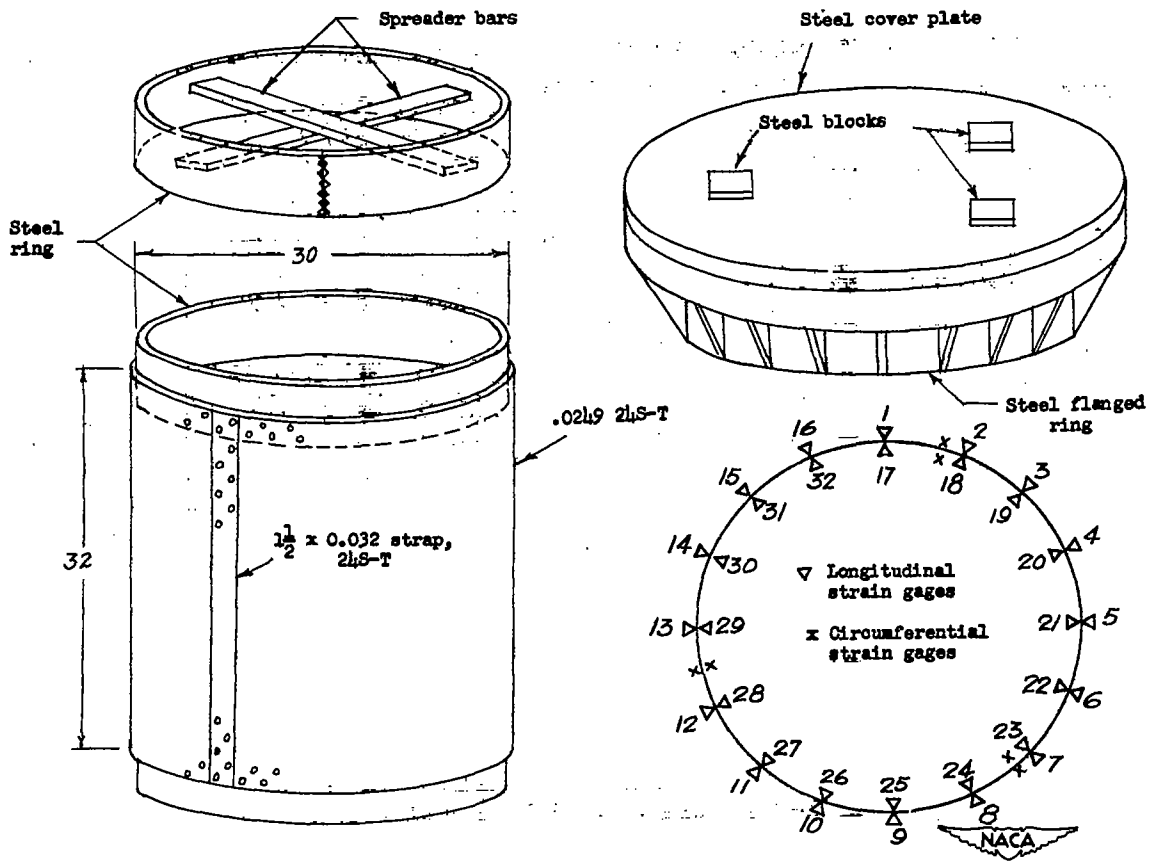

Figure 1.- Test specimen and strain-gage positions.

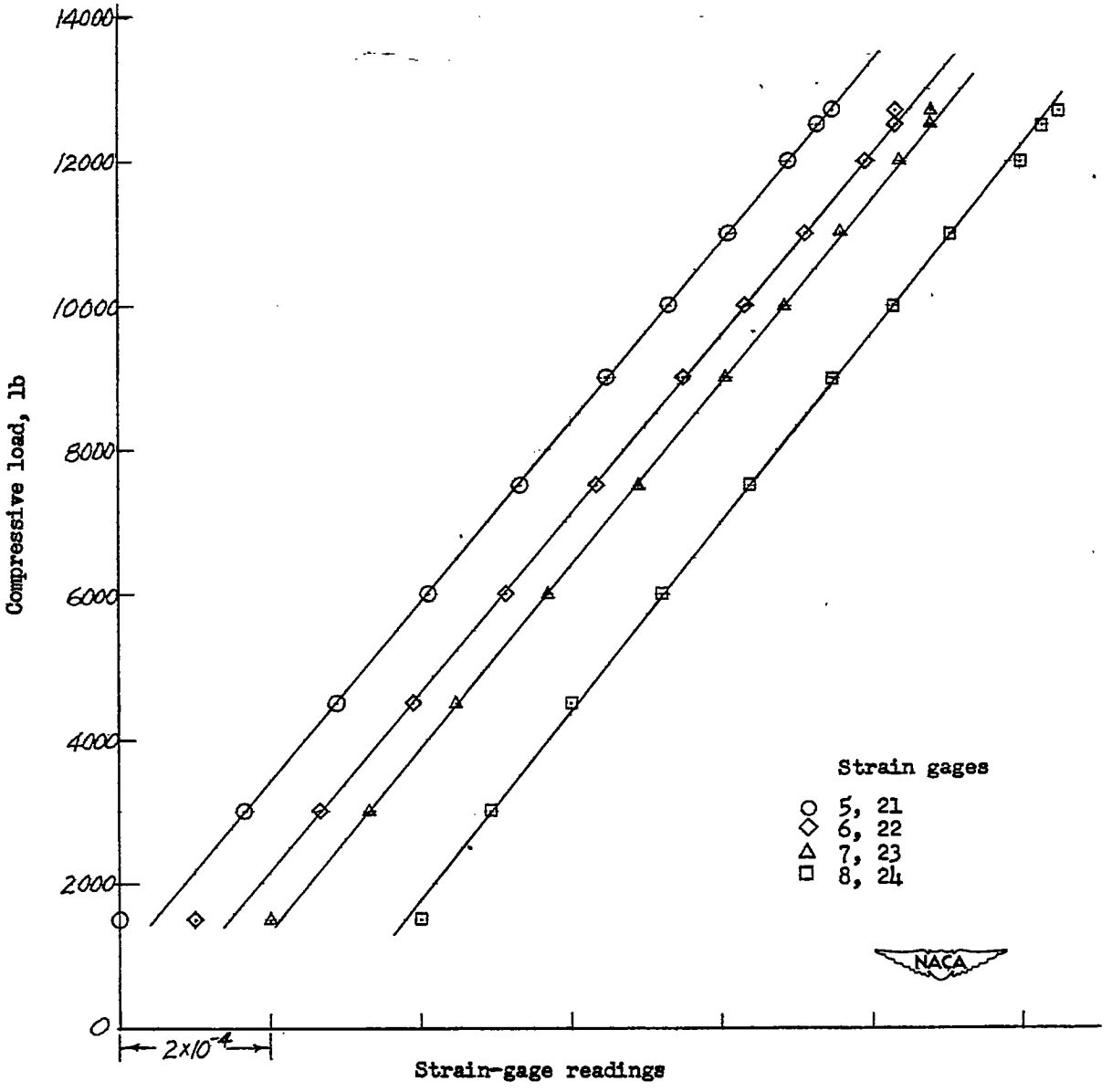

(a) Linear part of load-strain curve for four typical pairs of strain gages.

Figure 2.- Typical experimental result. Internal pressure, $1\frac{1}{2}$ psi.

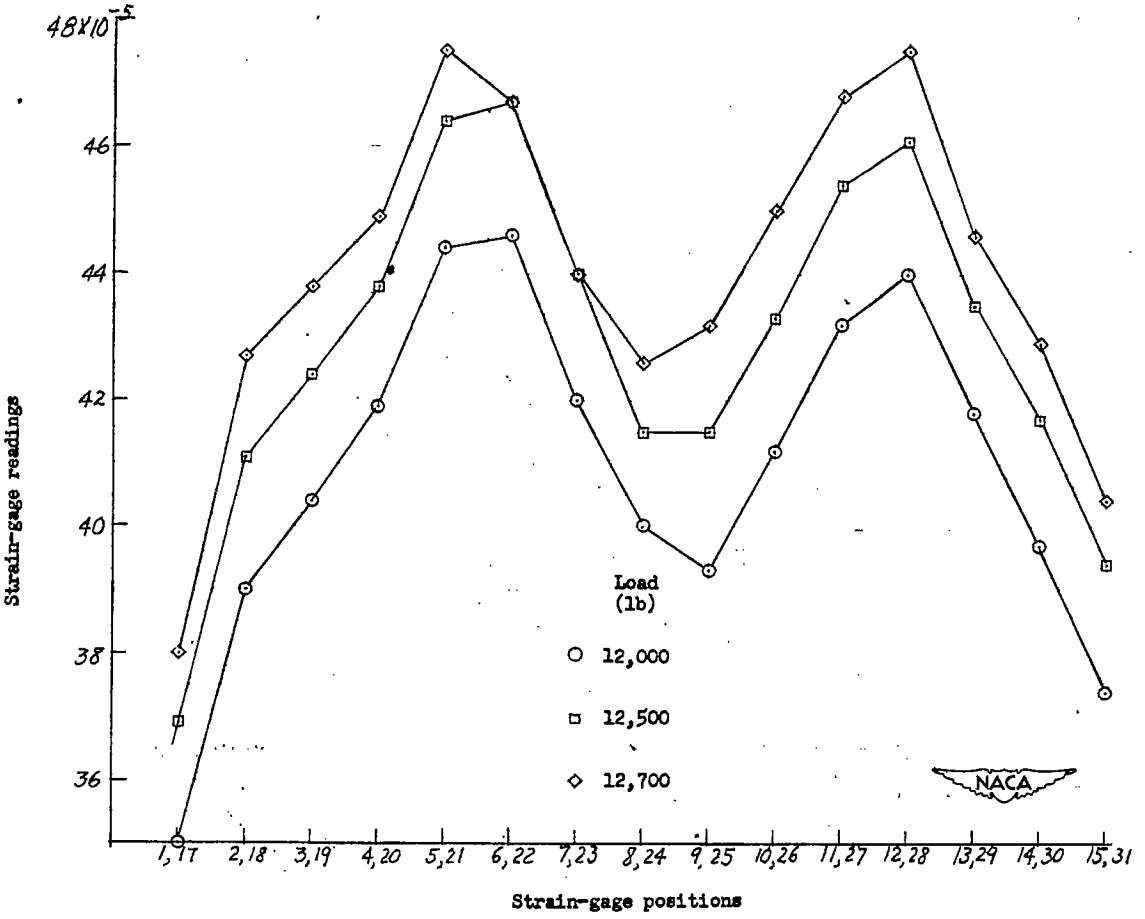

(b) Close to buckling load.

Figure 2.- Concluded.

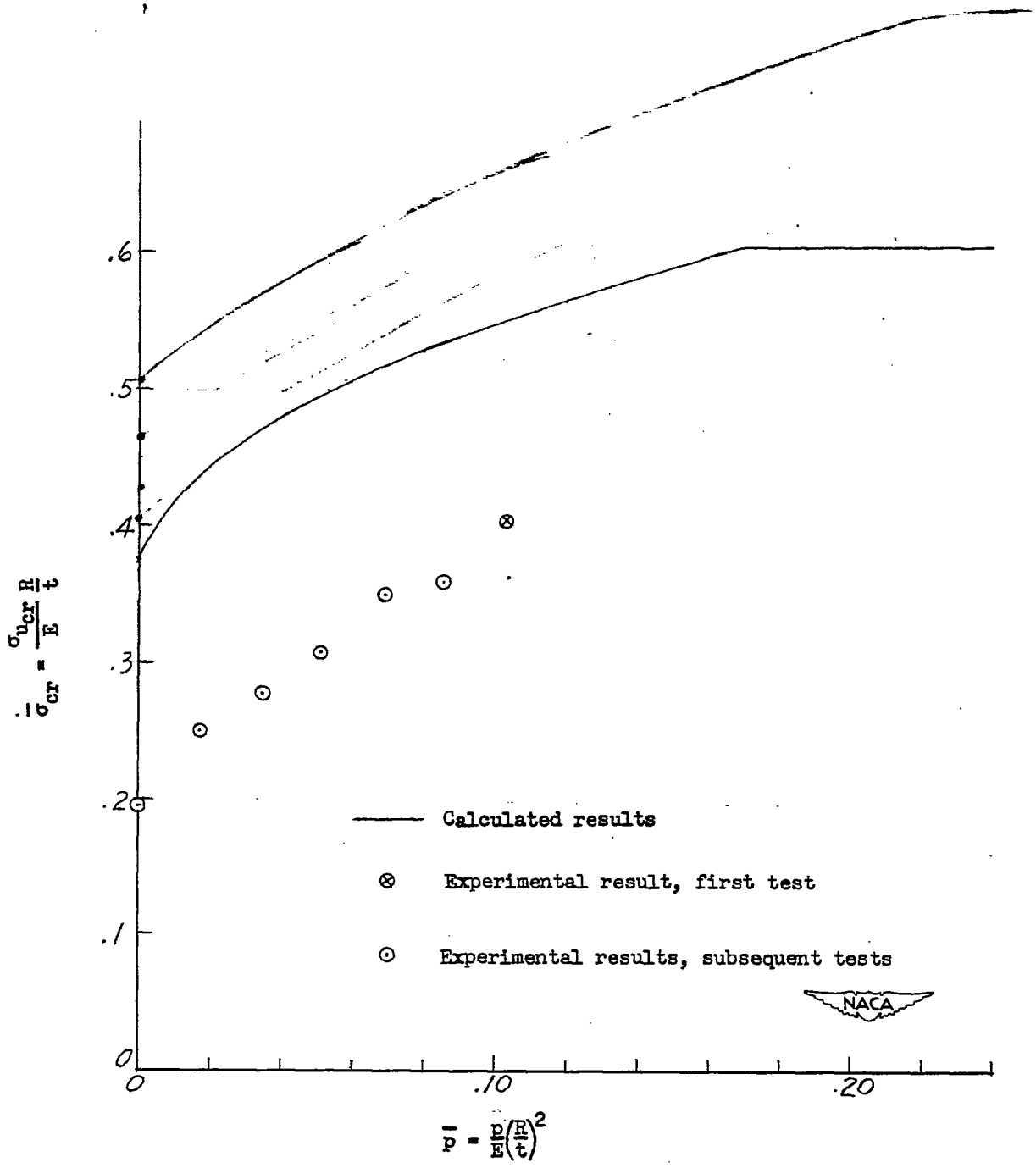

Figure 3.- Comparison of theoretical and experimental results of the buckling stress at various internal pressures.

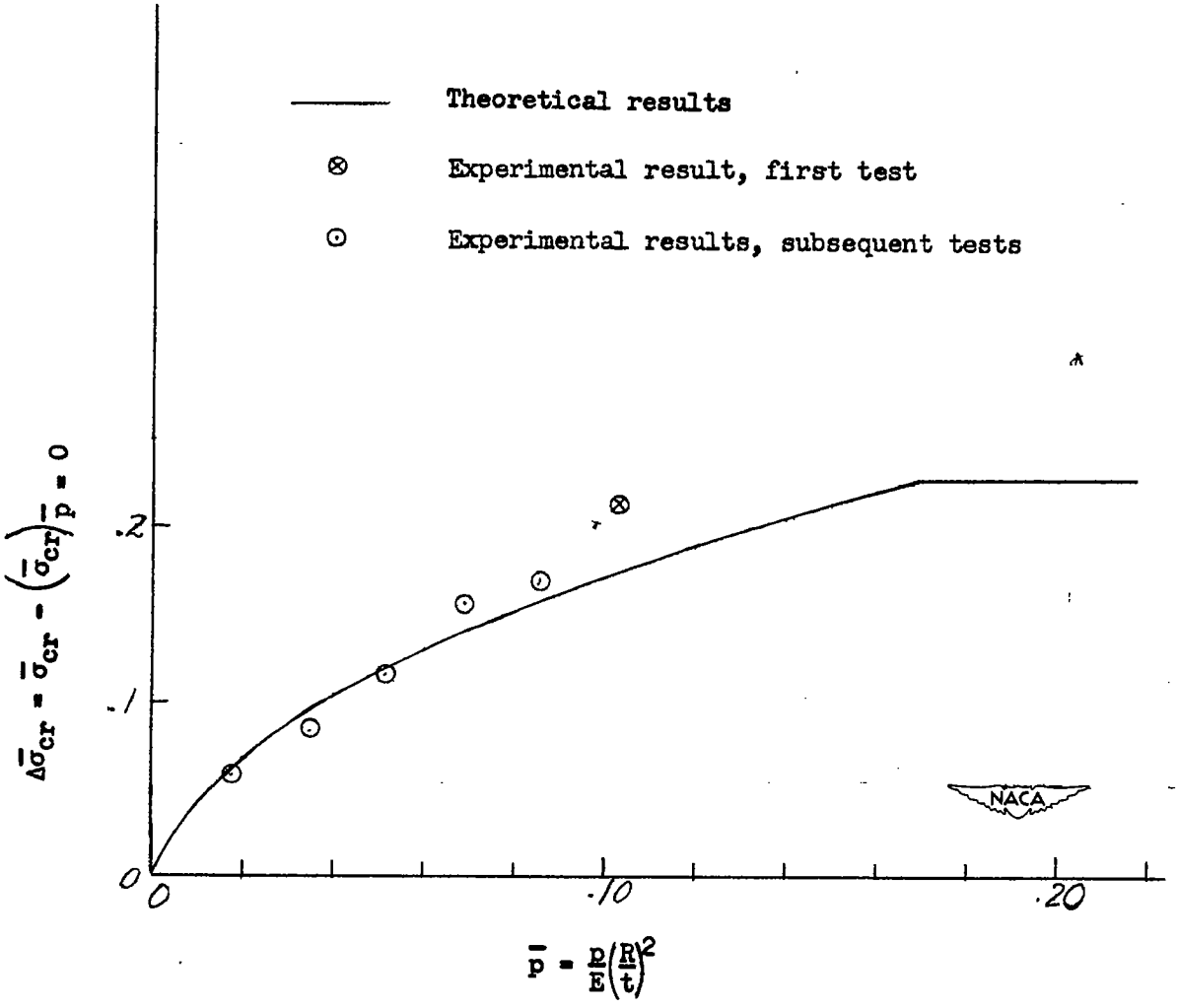

Figure 4.- Theoretical and experimental results showing the increment of buckling stress due to internal pressure.

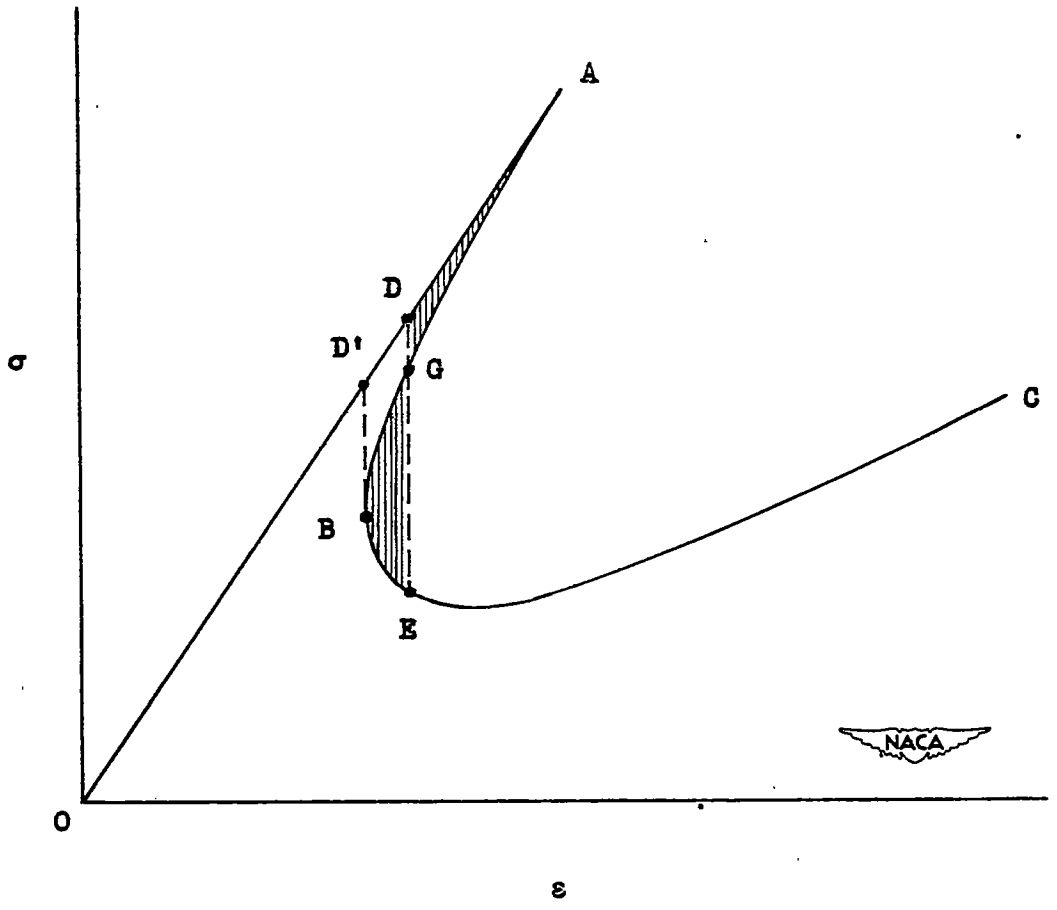

Figure 5.- Relation between the average compressive stress σ and the end-shortening ϵ.